Farnesoid x receptor deficiency improves glucose homeostasis in mouse models of obesity

Janne Prawitt [1] , Mouaadh Abdelkarim [1] , Johanna H. M. Stroeve [2] , Iuliana Popescu [1] , Helene Duez [1] , Vidya R. Velagapudi [3] , Julie Dumont [1] , Emmanuel Bouchaert [1] , Theo H. Van Dijk [2] , Anthony Lucas [1] , Emilie Dorchies [1] , Mehdi Daoudi [1] , Sophie Lestavel [1] , Frank J. Gonzalez [4] , Matej Oresic [3] , Bertrand Cariou [1 5 6] , Folkert Kuipers [2] , Sandrine Caron [1] , Bart Staels [1 *]

[1] *Récepteurs nucléaires, maladies cardiovasculaires et diabète INSERM : U1011 , Institut Pasteur de Lille , Université du Droit et de la Santé - Lille II , 1 rue du Prof Calmette 59019 Lille Cedex,FR*

[2] *Department of Pediatrics University of Groningen and University Medical Center Groningen , Center for Liver, Digestive and Metabolic Diseases , 9700 RB Groningen,NL*

[3] *VTT Technical Research Centre of Finland , 02150 Espoo, FI*

[4] *Laboratory of metabolism Center for Cancer Research , National Cancer Institute , National Institute of Health (NIH) , Bethesda 20892, US*

[5] *Institut du thorax INSERM : U915 , Université de Nantes , IFR26 , FR*

[6] *Clinique d'endocrinologie CHU Nantes , IFR26 , 1, place Alexis Ricordeau 44000 Nantes, FR*

[*] Correspondence should be adressed to: Bart Staels <bart.staels@pasteur-lille.fr >

Abstract

Objective

Bile acids (BA) participate in the maintenance of metabolic homeostasis acting through different signaling pathways. The nuclear BA receptor farnesoid X receptor (FXR) regulates pathways in BA, lipid, glucose and energy metabolism which become dysregulated in obesity. However, the role of FXR in obesity and associated complications, such as dyslipidemia and insulin resistance, has not been directly assessed.

Research Design and Methods

Here, we evaluate the consequences of FXR-deficiency on body weight development, lipid metabolism and insulin resistance in murine models of genetic and diet-induced obesity.

Results

FXR-deficiency attenuated body weight gain and reduced adipose tissue mass in both models. Surprisingly, glucose homeostasis improved due to an enhanced glucose clearance and adipose tissue insulin sensitivity. In contrast, hepatic insulin sensitivity did not change, and liver steatosis aggravated due to the repression of β-oxidation genes. In agreement, liver-specific FXR-deficiency did not protect from diet-induced obesity and insulin resistance indicating a role for non-hepatic FXR in the control of glucose homeostasis in obesity. Decreasing elevated plasma BA concentrations in obese FXR-deficient mice by administration of the BA sequestrant colesevelam improved glucose homeostasis in a FXR-dependent manner indicating that the observed improvements by FXR-deficiency are not due to indirect effects of altered BA metabolism.

Conclusions

Overall, FXR-deficiency in obesity beneficially affects body weight development and glucose homeostasis.

Author Keywords FXR ; bile acids ; obesity ; glucose homeostasis ; insulin resistance ; energy metabolism ; triglyceride metabolism ; bile acid sequestrants

Obesity is characterized by an excess of adipose tissue mass which predisposes to metabolic perturbations, including insulin resistance, hyperlipidemia and fatty liver, promoting the development of type 2 diabetes and cardiovascular disease. Dysregulation of various metabolic pathways in tissues such as adipose tissue, skeletal muscle, the pancreas and the liver lay at the basis of these metabolic complications, but the exact mechanisms are still not well understood (1).

Nuclear receptors are ligand-activated transcription factors, which regulate gene expression by binding to specific response elements in the promoters of target genes. The farnesoid X receptor (FXR) is a key regulator of bile acid (BA) metabolism. By promoting BA efflux from the liver, inhibiting hepatic BA synthesis and intestinal absorption, FXR controls the enterohepatic cycling of BA (2). Additionally, FXR regulates lipid metabolism, insulin sensitivity and energy homeostasis (3). FXR activation lowers plasma and liver triglycerides by repressing sterol regulatory element binding protein (SREBP)1c-mediated hepatic lipogenesis (4) and by enhancing plasma triglyceride

clearance via apolipoprotein (apo)CII induction (5) and apoCIII inhibition (6) in the liver, resulting in an increased lipoprotein lipase (LPL) activity. Consequently, FXR-deficient ($FXR^{-/-}$) mice are dyslipidemic, displaying elevated plasma triglycerides, total and HDL-cholesterol (7 –9).

The characterization of $FXR^{-/-}$ mice further revealed an important function of FXR in the control of glucose homeostasis. $FXR^{-/-}$ mice are transiently hypoglycemic when fasted (8 ,10), exhibit a delayed intestinal glucose absorption (10) and a reduced hepatic glycogen content (10 –12). Hepatic gluconeogenic gene expression is decreased in the absence of FXR (11 –13) and induced upon FXR activation *in vivo* (14). Moreover, $FXR^{-/-}$ mice display peripheral insulin resistance with an impaired insulin signaling response in adipose tissue and skeletal muscle (8 ,13). Additionally, FXR may control adipose tissue biology. $FXR^{-/-}$ mice exhibit a decrease in adipose tissue mass with smaller adipocytes (8). Conversely, FXR activation *in vitro* stimulates adipocyte differentiation (15) by promoting PPARγ activity and inhibiting the Wnt/β-catenin pathway (16).

BA act as regulators of metabolic homeostasis also through FXR-independent pathways (17). Apart from FXR, BA have been reported to activate the G-protein coupled BA receptor (TGR5), the pregnane X receptor (PXR), the vitamin D receptor (VDR) or the formyl peptide receptor (FPR) (17). TGR5 activation by BA increases energy expenditure in thermogenic tissues by inducing deiodinase 2 (D2) (18) and improves glucose homeostasis by stimulating glucagon-like peptide 1 (GLP-1) secretion from intestinal L-cells (19 ,20). Hence, since FXR controls plasma BA concentrations, the metabolic actions of FXR can be due to direct FXR-mediated and/or indirect BA-mediated effects (2). BA metabolism can be pharmacologically modulated by BA sequestrants (BAS), such as colesevelam, which bind BA in the intestinal lumen and interrupt their enterohepatic cycling. BAS lower plasma cholesterol levels by stimulating hepatic BA synthesis from cholesterol and increasing LDL receptor activity (3). In diabetic patients, BAS improve glycemic control (21), associated with an activation of the incretin system due to an enhanced GLP-1 secretion as shown in rodent models of diabetes (22 ,23).

Studies on the metabolic function of FXR have so far been limited to lean $FXR^{-/-}$ mice. However, the role of FXR in the adaptation to obesity and its metabolic complications has not yet been assessed. To address this issue, we investigated the impact of FXR-deficiency in murine models of genetic (ob/ob) and diet-induced obesity. Our results show that FXR-deficiency protects from excessive body weight gain in both models by reducing adipose tissue mass. Interestingly, hyperglycemia and glucose tolerance improved associated with improved peripheral glucose clearance and adipose tissue insulin sensitivity. Liver insulin sensitivity was not altered by FXR-deficiency and hepatic steatosis became even more pronounced associated with elevated plasma triglyceride levels and reduced expression of genes implicated in β-oxidation. Furthermore, liver-specific FXR-deficient mice were not protected from diet-induced obesity and insulin resistance, indicating a role for non-hepatic FXR in the improvement of glucose metabolism. Finally, to assess the contribution of elevated plasma BA concentrations observed in FXR-deficient models of obesity, plasma BA levels were reduced by administration of the BAS colesevelam. Colesevelam treatment improved glucose homeostasis in genetic obesity only in the presence of FXR, indicating that the changes in BA concentrations are not responsible for the improved glucose homeostasis in obese FXR-deficient mice. Thus, selective FXR antagonism or elimination of ligands, e.g. by BAS, may be an interesting pharmacological option for the therapy of metabolic disorders associated with obesity.

Research Design and Methods

Animals

All experiments were performed with the approval of the Institut Pasteur de Lille review board. Animals were housed in a 12h-light/12h-dark cycle and maintained on a standard chow (A03, SAFE). Unless stated otherwise, male mice were used for experimentation. $FXR^{-/-}$ (7) and FXR-floxed mice (7) were backcrossed for seven or ten generations, respectively, onto a C57Bl/6J background. $FXR^{+/+}$ ob/ob and $FXR^{-/-}$ ob/ob mice and lean littermates were generated by crossing $FXR^{-/-}$ and leptin-deficient mice (B6.V-Lep ^{ob} /J, Charles River). Liver-specific $FXR^{-/-}$ mice ($FXR^{flox/flox}$ Alb-$Cre^{+/-}$ =$LFXR^{-/-}$) and wildtype littermates ($FXR^{flox/flox}$ Alb-$Cre^{-/-}$ =$LFXR^{+/+}$) were generated by crossing FXR-floxed and Albumin-Cre recombinase expressing mice (C57BL/6-Tg(Alb-cre)21Mgn/J, Charles River). To study diet-induced obesity, mice received a high-fat diet (HFD) (D12492, Research Diets; 60% kcal fat) and controls a low-fat diet (D12450B, Research Diets; 10% kcal fat), 20w-old $FXR^{+/+}$ and $FXR^{-/-}$ mice for 20w and 10w-old $LFXR^{-/-}$ and $LFXR^{+/+}$ mice for 9w. The BAS colesevelam (Daiichi Sankyo) was administered with the diet (2% in standard chow) ad libitum to 10w-old $FXR^{+/+}$ ob/ob and $FXR^{-/-}$ ob/ob mice for 3w. Body weight was monitored weekly. Fat and lean mass were determined by dual x-ray absorptiometry (Piximus, GE Medical Systems LUNAR). Food intake was estimated during 6 periods of 2d. Animals were sacrificed after a 6h-fast by cervical dislocation. Tissues were removed and snap-frozen in liquid nitrogen.

Plasma parameters

Blood was sampled after a 6h-fast and parameters determined as followed: blood glucose (Accu-Check, Roche Diagnostics), insulin (Mercodia), non-esterified fatty acids (FFA) (Wako), triglycerides (Biomerieux), leptin (R&D Systems) and total BA as described (24). Lipoprotein profiles in plasma pools were generated by fast protein liquid chromatography (FPLC; Superose 6 HR 10/30, Amersham GE Healthcare) with subsequent determination of triglycerides.

Indirect calorimetry

Mice were housed individually in metabolic cages (Oxylet, PanLab) for 48h to measure O_2 -consumption (V_{O2}) and CO_2 -production (V_{CO2}). Energy expenditure was calculated as described (25).

VLDL production

Mice were intravenously injected with 500mg/kg Tyloxapol (Sigma) after a 6h-fast and triglycerides were measured in plasma sampled as indicated.

Assessment of glucose metabolism

For tolerance tests 1g/kg glucose or 2IU/kg insulin (Actrapid Penfill, Novo Nordisk), respectively, were injected intraperitoneally and blood glucose measured as indicated. The metabolic clearance rate (MCR) was determined by stable isotope dilution as described (26). To measure the insulin signaling response, tissues were harvested 10min after intraperitoneal injection of 1IU/kg insulin (Actrapid Penfill, Novo Nordisk) or 0.9% NaCl into overnight-fasted female mice. Serine473-phosphorylated Akt and total Akt protein expression (Cell Signaling Technology) were detected by Western Blot and signals quantified by GeneTool software (Syngene). Pancreas morphometry was analyzed as described (27).

Quantitative RT-PCR (qPCR)

Total RNA was isolated from tissue samples by GSCN/phenol/chloroform extraction (28) and reverse transcribed into cDNA (Superscript II kit, Applied Bioscience). QPCR was performed with the BrilliantII SYBR Green QPCR Master Mix (Agilent) and specific primers (Supplementary Table 1) on a mx3005 (Agilent). Gene expression was normalized to 28S and the value in $FXR^{+/+}$ ob/ob samples set to 1.

Lipidomics

Lipidomics analysis of adipose tissue was performed as described (29).

Statistical analysis

All values are reported as means±SEM. Statistical significance was analyzed as indicated by 2way-ANOVA and Bonferroni posthoc test or Mann-Whitney test using Prism (GraphPad). Differences were considered significant when $p<0.05$. Partial least squares discriminant analysis (PLS/DA) was performed using Matlab, version 7.5 (Mathworks) and PLS Toolbox, version 4.2 (Eigenvector Research).

Results

FXR-deficiency attenuates weight gain in genetic obesity

As a first approach to assess the role of FXR in obesity, $FXR^{-/-}$ mice were crossed into the ob/ob background to produce $FXR^{-/-}$ ob/ob mice which were subsequently compared to $FXR^{+/+}$ ob/ob controls.

The weight gain observed in $FXR^{+/+}$ ob/ob mice was significantly attenuated by FXR-deficiency, already from 7w of age onwards (Fig. 1A) ($p<0.0001$; 2way-ANOVA). Dual x-ray absorptiometry revealed a decrease in fat (22%) and less pronounced in lean (10%) mass of $FXR^{-/-}$ ob/ob mice (Fig. 1B). Concordantly, the estimated food intake tended to decrease in $FXR^{-/-}$ ob/ob mice (15.5±1.1 vs. 18.9±0.8 kcal/d/mouse). Indirect calorimetry demonstrated that O_2 -consumption (V_{O2}) and CO_2 -production (V_{CO2}) were equally reduced in $FXR^{-/-}$ ob/ob mice compared to $FXR^{+/+}$ ob/ob controls (Fig. 1C and 1D), resulting in nearly identical values for the respiratory quotient (data not shown). Consistent with the decrease in V_{O2} and body weight, calculated energy expenditure was lower in $FXR^{-/-}$ ob/ob than in $FXR^{+/+}$ ob/ob mice (7.1±0.3 vs. 8.7±0.7 kcal/d/mouse) even though the difference did not reach statistical significance.

Overall, FXR-deficiency leads to a decreased storage of energy in form of adipose tissue resulting in a lower total body weight.

FXR-deficiency improves glucose homeostasis in genetic obesity by increasing peripheral glucose disposal

Since lean FXR$^{-/-}$ mice develop peripheral insulin resistance (8 ,13), it was next assessed whether FXR-deficiency in obesity affects glucose homeostasis. In contrast to hyperglycemic FXR$^{+/+}$ ob/ob mice, FXR$^{-/-}$ ob/ob mice displayed normal blood glucose levels (Fig. 2A) ($p<0.0001$; 2way-ANOVA). In addition, the hyperinsulinemia typically observed in FXR$^{+/+}$ ob/ob mice was significantly reduced in the absence of FXR (Fig. 2B). Concordant with the decreased hyperglycemia and hyperinsulinemia, glucose tolerance was significantly improved in FXR$^{-/-}$ ob/ob mice (Fig. 2C), due to a combination of lower fasting glycemia and improved glucose handling as evident from the significantly smaller integrated area under the curve (iAUC) (Fig. 2D). The MCR of glucose was further significantly improved in FXR$^{-/-}$ ob/ob mice (Fig. 2E) indicative of a higher glucose disposal in the periphery. In line, an insulin tolerance test showed that FXR$^{-/-}$ ob/ob mice are more insulin sensitive than FXR$^{+/+}$ ob/ob mice (Fig. 2F and 2G) with a more drastic decline of blood glucose levels in response to the administered insulin bolus ($p<0.0001$; 2way-ANOVA). Insulin resistant FXR$^{+/+}$ ob/ob mice exhibited enlarged islets of Langerhans (Fig. 2H , compare arrows) due to compensatory hypertrophy. In contrast, islets of FXR$^{-/-}$ ob/ob mice were significantly smaller likely (Fig. 2I) reflecting the relieved metabolic pressure due to the improved insulin sensitivity. These findings indicate that, in contrast to lean mice, FXR-deficiency might improve glucose homeostasis in genetic obesity.

Adipose tissue, but not hepatic insulin sensitivity is improved in FXR$^{-/-}$ ob/ob mice

To analyze the contribution of peripheral tissues and the liver to the improvement of insulin sensitivity, the phosphorylation of Akt, a key mediator of insulin's metabolic action, was measured in response to an *in vivo* administered insulin bolus (Fig. 3A). Akt phosphorylation was increased in adipose tissue of FXR$^{-/-}$ ob/ob compared to FXR$^{+/+}$ ob/ob mice (2.8x vs. 1.5x). In contrast, the response in skeletal muscle (4.5x vs. 4.8x) and liver (2.0x vs. 1.7x) was not different between both genotypes.

Hepatic insulin resistance is often associated with a fatty liver (30). Since FXR regulates lipogenesis in lean mice (2), hepatic gene expression and lipid content were determined. No changes were seen in the mRNA expression of the key regulator of lipogenesis, SREBP1c (Fig. 3B). Expression of genes involved in FA synthesis were only modestly induced (ACC1, FAS, SCD1) in livers of FXR$^{-/-}$ ob/ob mice (Fig. 3B). Nevertheless, the hepatic triglyceride content was doubled in the absence of FXR (Fig. 3C). The expression of PPARα, a key regulator of FA oxidation, and CPT1A, which ensures the FA entry into the mitochondria, were significantly decreased in FXR$^{-/-}$ ob/ob compared to FXR$^{+/+}$ ob/ob mice (Fig. 3B). Expression of ACC2, which indirectly inhibits CPT1A, was significantly higher, indicating that a reduced FA oxidation likely contributes to the increased steatosis in FXR$^{-/-}$ ob/ob mice. Thus, an improvement of adipose tissue insulin sensitivity seems to account for the observed changes in glucose homeostasis. Hepatic insulin sensitivity was not altered by FXR-deficiency, even though liver steatosis increased.

FXR$^{-/-}$ ob/ob mice exhibit hypertriglyceridemia due to an impaired intravascular triglyceride clearance

Since FXR$^{-/-}$ ob/ob mice display increased liver steatosis and reduced adipose tissue mass, it was tested whether this phenotype was associated with alterations in triglyceride or FA metabolism. Plasma FFA concentrations were not different between genotypes (Fig. 4A). In contrast, plasma triglyceride levels were strongly elevated in FXR$^{-/-}$ ob/ob compared to FXR$^{+/+}$ ob/ob mice (Fig. 4B). Analysis of the lipoprotein profile revealed that triglycerides were mainly increased in VLDL, but also IDL/LDL-sized particles (Fig. 4C). To determine whether this was due to altered hepatic triglyceride secretion, plasma triglyceride accumulation was assessed after inhibition of intravascular lipolysis (Fig. 4D). Hepatic VLDL production was similar between FXR$^{-/-}$ ob/ob and FXR$^{+/+}$ ob/ob mice, suggesting that an impairment of intravascular triglyceride clearance by LPL underlies the elevated plasma triglycerides. Consistently, hepatic mRNA levels of apoCII and apoAV, activators of LPL, were markedly repressed (by 65% and 74%, respectively) in FXR$^{-/-}$ ob/ob mice (Fig. 4E). Hence, the repression of plasma triglyceride clearance regulators combined with the reduction of adipose tissue mass might result in the development of hypertriglyceridemia.

Total but not liver-specific FXR-deficiency protects from diet-induced obesity and insulin resistance

To assess the impact of FXR-deficiency in obesity in a model expressing functional leptin, lean FXR$^{-/-}$ and FXR$^{+/+}$ mice were fed a HFD for 20w. Whereas FXR$^{+/+}$ mice rapidly gained weight upon HFD-feeding, body weight remained significantly lower in FXR$^{-/-}$ mice (Fig. 5A). Consistently, plasma leptin levels were lower in FXR$^{-/-}$ mice (Fig. 5B). Plasma triglycerides were significantly higher in FXR$^{-/-}$ mice upon HFD-feeding (Fig. 5C). FXR$^{-/-}$ mice further displayed lower blood glucose (Fig. 5D) and plasma insulin (Fig. 5E) concentrations and showed an improved glucose tolerance ($p<0.0001$; 2way-ANOVA) (Fig. 5F and G). Hence, similar as in ob/ob mice, FXR-deficiency protects from diet-induced obesity and insulin resistance.

To determine the contribution of hepatic FXR to the protection from diet-induced obesity and insulin resistance, liver-specific FXR$^{-/-}$ mice (LFXR$^{-/-}$) and wildtype littermates (LFXR$^{+/+}$) were fed a HFD for 9w. Both LFXR$^{-/-}$ and LFXR$^{+/+}$ mice developed obesity (Fig. 6A) and displayed significantly elevated plasma leptin levels upon HFD-feeding (Fig. 6B). LFXR$^{-/-}$ mice had significantly higher basal plasma triglycerides than LFXR$^{+/+}$ littermates but were unaffected by HFD-feeding (Fig. 6C). HFD-fed LFXR$^{-/-}$ and LFXR$^{+/+}$ mice

became insulin resistant displaying hyperglycemia (p<0.0001; 2way-ANOVA) (Fig. 6D) and elevated plasma insulin levels (Fig. 6E). In addition, the diet-induced glucose intolerance was similar in both genotypes (Fig. 6F and 6G). These findings indicate that liver-specific FXR-deficiency does not protect from diet-induced obesity and insulin resistance.

Modulation of BA metabolism by sequestration does not affect glucose homeostasis in $FXR^{-/-}$ ob/ob mice

FXR-deficiency led to elevated plasma BA concentrations in genetic (394±86μM vs. 44±13μM, p<0.001) and diet-induced obesity (119±50μM vs. 22±6μM). Since BA exert regulatory functions independent of FXR (17), we evaluated whether this increase may account for the observed alteration of body weight and glucose homeostasis.

The increased availability of plasma BA may lead to the activation of the TGR5 signaling pathway subsequently increasing energy expenditure in brown adipose tissue (BAT) (18). However, the expression of the TGR5 target genes UCP1 and D2 was decreased or unchanged, respectively, in BAT of $FXR^{-/-}$ ob/ob compared to $FXR^{+/+}$ ob/ob mice (Fig. 7A), indicating that TGR5 activity was not induced.

To assess whether reducing the elevated plasma BA levels in $FXR^{-/-}$ ob/ob mice would affect glucose homeostasis, the BAS colesevelam was administered to $FXR^{-/-}$ ob/ob and $FXR^{+/+}$ ob/ob mice for 3w. Colesevelam successfully reduced plasma BA concentrations in both genotypes by around 80% already within 9d of treatment (Fig. 7B). Body weight slightly but significantly increased with colesevelam treatment only in $FXR^{-/-}$ ob/ob mice (Fig. 7C). Colesevelam decreased blood glucose levels in $FXR^{+/+}$ ob/ob, but not $FXR^{-/-}$ ob/ob mice (Fig. 7D). The glucose intolerance observed in untreated $FXR^{+/+}$ ob/ob mice improved upon colesevelam treatment, whereas such effect was not observed in $FXR^{-/-}$ ob/ob mice (Fig. 7E and 7F). However, both genotypes displayed increased plasma insulin concentrations upon treatment (Fig. 7G). Since BAS may lower glycemia by activating the incretin system (23), the expression of implicated intestinal genes was measured (Supplementary Table 2). The expression of proglucagon, coding for GLP-1, and ProGIP, coding for GIP, were induced and repressed, respectively, by FXR-deficiency. However, only PC1/3, the enzyme activating both incretins, was moderately induced by colesevelam in $FXR^{+/+}$ ob/ob mice, unlikely explaining the observed improvement of glucose homeostasis. Thus, reducing plasma BA concentrations had no effect on glucose homeostasis in the absence of FXR, suggesting that the alterations of glucose metabolism observed in FXR-deficiency are not mediated by circulating BA.

FXR-deficiency differentially affects the abundance of long- and medium-chain triglyceride species in adipose tissue of lean and ob/ob mice

FXR-deficiency improves glucose homeostasis in obesity, due at least in part to an increase in adipose tissue insulin sensitivity. To investigate changes in adipose tissue lipid composition linked to FXR-deficiency before the metabolic phenotype fully develops, high-resolution lipidomics was performed in subcutaneous adipose tissue from 6w-old lean and ob/ob (obese) $FXR^{-/-}$ and $FXR^{+/+}$ mice.

Overall, 133 lipid species were quantified. Total phospholipid and sphingomyelin content was significantly lower in obese than in lean mice, whereas total triglycerides were similar (Supplementary Fig. 1). These lipid classes were unaffected by FXR-deficiency. Of interest, a number of triglyceride species was differentially affected by FXR-deficiency in lean and obese mice. The concentration of medium-chain triglycerides with a high saturation level was significantly higher in obese than lean $FXR^{+/+}$ mice (Fig. 8A–C) and tended to increase by FXR-deficiency in both. In contrast, long-chain, unsaturated triglycerides were also significantly elevated in obese compared to lean $FXR^{+/+}$ mice, however increased by FXR-deficiency in lean but decreased in obese mice (Fig. 8D–F). Further, long-chain triglycerides containing few double-bounds, which were similar between lean and obese $FXR^{+/+}$ mice, only decreased by FXR-deficiency in lean mice (Fig. 8G–I).

PLS/D analysis revealed that the global subcutaneous adipose tissue lipid profiles clustered according to their genotype (Fig. 8J). Lipid profiles are significantly different between lean and obese mice whether deficient or not for FXR, visualized as a clear separation by the latent variable (LV)1 plotted on the x-axis. Interestingly, the LV2 demonstrated an additional separation of lean $FXR^{+/+}$ and obese $FXR^{-/-}$ from lean $FXR^{-/-}$ and obese $FXR^{+/+}$ mice, indicating that FXR-deficiency modulates lipid profiles in an opposite manner in the lean versus obese background.

Discussion

The nuclear receptor FXR is a metabolic regulator which controls BA and lipid as well as glucose and energy metabolism (2). FXR can exert direct transcriptional control or indirectly influence metabolic pathways by modulating the homeostasis of BA, which control metabolism also independent of FXR (17). The characteristics of $FXR^{-/-}$ mice - dyslipidemia (7 –9), transient hypoglycemia upon fasting (8 ,10), peripheral insulin resistance (8 ,13) and reduced adipose tissue mass (8 ,15) - reflect the importance of FXR for the maintenance of metabolic homeostasis. Yet, the impact of FXR-deficiency on obesity and associated metabolic disorders has not been assessed. In the current study we demonstrate, that FXR-deficiency in murine models of genetic and diet-induced obesity attenuated weight gain by

reducing adipose tissue mass. FXR-deficiency further improved glucose homeostasis by enhancing peripheral glucose disposal and increasing adipose tissue insulin sensitivity. This improvement is not mediated by hepatic FXR, since liver insulin sensitivity was unchanged and liver-specific $FXR^{-/-}$ mice were not protected from diet-induced obesity and insulin resistance. The administration of the BAS colesevelam, which reduced the elevated plasma BA levels resulting from FXR-deficiency in obesity, further revealed that the improved glucose homeostasis was independent of BA-mediated pathways. FXR-deficiency thus exerts a beneficial effect on body weight development and glucose homeostasis in obesity.

$FXR^{-/-}$ mice display peripheral insulin resistance, but reported results on the liver are contradicting (8 ,13 ,31). Surprisingly, we observed an improvement of glucose homeostasis by FXR-deficiency in genetic and diet-induced obesity, revealing a differential role for FXR in glucose homeostasis in basal (lean) and challenged (obese) metabolic conditions. The reduction of hyperglycemia in $FXR^{-/-}$ ob/ob mice resulted from an increased peripheral glucose disposal associated with an improved adipose tissue insulin sensitivity. This suggests that FXR in adipose tissue contributes to the dysregulation of glucose metabolism in obesity. Hypertrophic adipocytes develop insulin resistance (32). Hence the reduced adipocyte size in $FXR^{-/-}$ ob/ob mice (16) might explain the increased insulin sensitivity. In addition to adipose tissue, skeletal muscle is the main peripheral tissue accounting for glucose uptake. However, the insulin signaling response in skeletal muscle was unaffected by FXR-deficiency. Moreover, FXR is not expressed in skeletal muscle (8) and muscle mass strongly reduced in genetic obesity. We can therefore exclude the involvement of skeletal muscle in the FXR-deficiency- mediated changes of glucose homeostasis.

FXR exerts a key function in the control of hepatic glucose and lipid metabolism (2). In hepatic insulin resistance, increased endogenous glucose production contributes to hyperglycemia and the continuous insulin-mediated activation of lipogenesis leads to hyperlipidemia and may cause a fatty liver (32). In contrast to adipose tissue, FXR-deficiency did not improve hepatic insulin sensitivity in genetic obesity and liver-specific FXR-deficiency did not protect from diet-induced insulin resistance, a rather surprising result regarding the importance of hepatic FXR for the metabolic control of lean mice. Further, hepatic steatosis often associated with hepatic insulin resistance increased in $FXR^{-/-}$ ob/ob mice due to a repression of β-oxidation. Moreover, the repression of hepatic LPL cofactors led to an impaired intravascular triglyceride clearance resulting in elevated plasma triglycerides. Overall, the changes in lipid metabolism appear to be primarily due to altered liver function, while the results on insulin sensitivity emphasize a role for non-hepatic FXR in the dysregulation of glucose homeostasis in obesity - most probably in adipose tissue.

Several studies have shown that FXR controls adipocyte differentiation and function (8 ,15 ,16). FXR expression occurs early and transiently during adipocyte development, inhibiting the Wnt/β-catenin pathway, thus allowing optimal PPARγ activation (16). Since the lack of hepatic FXR does not seem to mediate the improvement of glucose homeostasis in obesity, it would be of great interest to study adipose tissue-specific FXR-deficiency in obesity. Unfortunately, in the currently available mouse models Cre recombinase expression is driven by promoters from late and/or non-specific adipocyte genes (i.e. adiponectin or aP2), rendering them inappropriate to study the influence of genes acting earlier in the differentiation process, such as FXR.

FXR-deficiency in obesity was associated with elevated plasma BA levels. BA have been reported to improve glucose homeostasis independent of FXR by TGR5-mediated stimulation of GLP-1 secretion (19 ,20). The administration of the BAS colesevelam to ob/ob mice successfully reduced plasma BA concentrations, but had no effect on glucose homeostasis in the absence of FXR. Thus, elevated circulating BA in FXR-deficiency do not mediate the observed improvement in glucose homeostasis. BAS improve glycemic control in type 2 diabetes, partly via a TGR5-mediated increase of GLP-1 secretion (22 ,23). The observed FXR-dependent improvement of glycemic control by colesevelam in ob/ob mice suggests that FXR-mediated pathways contribute to the beneficial effect of BAS.

Contradictory to our observation that FXR-deficiency is beneficial for glucose homeostasis in obesity, FXR activation has been shown to improve insulin resistance in rodent models of diabetes (8 ,31 ,33). The reason for this apparent inconsistency is currently unclear. However, the pharmacological activation of a nuclear receptor does not always and necessarily have the opposite effects than the knockout of its expression. The specific pharmacodynamics of the used compounds may also affect FXR in tissue-specific manner (sBARM effect), whereas our study focused on whole-body FXR-deficiency.

Both genetic and diet-induced obesity are attenuated in the absence of FXR. FXR-deficiency leads to reduced adipose tissue mass (8 , 15 ,16) and adipocyte size (16) in lean and ob/ob mice limiting energy storage capacity. Since food intake and energy expenditure only tended to decrease in $FXR^{-/-}$ ob/ob mice, the decreased adipose tissue mass most likely accounts for the reduced weight gain. With regard to the moderate decrease in energy expenditure, a central effect of FXR seems unlikely, additionally since FXR expression in hypothalamus is only very weak (34). Further, the lack of TGR5 target gene induction in BAT of $FXR^{-/-}$ ob/ob mice argues against the implication of a TGR5-cAMP-D2-mediated mechanism (18). If the reduced body weight was a direct effect of a decreased food intake in the hyperphagic model of $FXR^{-/-}$ ob/ob mice, the hepatic triglyceride content would have also been reduced and not elevated as observed.

Interestingly, the analysis of adipose tissue lipid profiles by lipidomics revealed a differential alteration of certain triglyceride classes in lean and obese mice by FXR-deficiency, e.g. long-chain, unsaturated triglycerides are lowered by FXR-deficiency in obese but increased in lean mice. This observation demonstrates that FXR-deficiency specifically and opposingly affects adipose tissue metabolism as it does glucose homeostasis in lean and obese conditions. Overall, in contrast to lean mice, FXR-deficiency in obesity improves energy and glucose homeostasis. The selective inhibition of FXR activity may thus be an appealing option for the therapy of obesity and the related dysregulation of glucose homeostasis.

Acknowledgements:

This study was supported by the EU Grant HEPADIP (N° 018734), the Agence Nationale de la Recherche (No.A05056GS) and COST (Action BM0602). We are grateful to Daiichi Sankyo for providing colesevelam and an unrestricted scientific grant.

Footnotes:

Author Contributions J.P. performed experiments and wrote the manuscript. M.A., J.H.M.S., I.R.P., H.D., V.R.V., J.D., E.B., T.H.vD., A.L., E.D. and M.D. performed experiments and contributed to discussion. B.C. and S.C. performed experiments, contributed to discussion and reviewed the manuscript. F.J.G., M.O. and F.K. contributed to discussion and reviewed the manuscript. B.S. contributed to discussion and wrote, reviewed and edited the manuscript.

Abbreviations

ACC : acetyl CoA carboxylase
ap2 : adipocyte lipid binding protein
Apo : apolipoprotein
BA : bile acid
BAS : bile acid sequestrant
BAT : brown adipose tissue
CPT1A : carnithin palmitoyl transferase 1A
D2 : deiodinase 2
FAS : fatty acid synthase
FFA : free fatty acid
FXR : farnesoid X receptor
GIP : glucose-dependent insulinotropic polypeptide
GLP-1 : glucagon-like peptide 1
HFD : high-fat diet
iAUC : integrated area under the curve
IDL : intermediary density lipoprotein
LPL : lipoprotein lipase
LV : latent variable
MCR : metabolic clearance rate
PC1/3 : proconvertase 1
PLS/DA : partial least squares discriminant analysis
PPARα : peroxisome proliferator-activated receptor α
SCD1 : stearoyl CoA desaturase 1
SREBP1c : sterol regulatory element binding protein 1c
TG : triglyceride
TGR5 : G protein-coupled bile acid receptor 1
UCP1 : uncoupling protein 1

References:

- 1 . Cornier M , Dabelea D , Hernandez TL . The metabolic syndrome . Endocr Rev . 2008 ; 29 : 777 - 822
- 2 . Lefebvre P , Cariou B , Lien F . Role of bile acids and bile acid receptors in metabolic regulation . Physiol Rev . 2009 ; 89 : 147 - 191
- 3 . Prawitt J , Caron S , Staels B . How to modulate FXR activity to treat the Metabolic Syndrome . Drug Discov Today Dis Mech . 2009 ; 6 : e55 - e64
- 4 . Watanabe M , Houten SM , Wang L . Bile acids lower triglyceride levels via a pathway involving FXR, SHP, and SREBP-1c . J Clin Invest . 2004 ; 113 : 1408 - 1418
- 5 . Kast HR , Nguyen CM , Sinal CJ . Farnesoid X-activated receptor induces apolipoprotein C-II transcription: a molecular mechanism linking plasma triglyceride levels to bile acids . Mol Endocrinol . 2001 ; 15 : 1720 - 1728
- 6 . Claudel T , Inoue Y , Barbier O . Farnesoid X receptor agonists suppress hepatic apolipoprotein CIII expression . Gastroenterology . 2003 ; 125 : 544 - 555
- 7 . Sinal CJ , Tohkin M , Miyata M . Targeted disruption of the nuclear receptor FXR/BAR impairs bile acid and lipid homeostasis . Cell . 2000 ; 102 : 731 - 744
- 8 . Cariou B , van Harmelen K , Duran-Sandoval D . The farnesoid X receptor modulates adiposity and peripheral insulin sensitivity in mice . J Biol Chem . 2006 ; 281 : 11039 - 11049
- 9 . Lambert G , Amar MJA , Guo G . The farnesoid X-receptor is an essential regulator of cholesterol homeostasis . J Biol Chem . 2003 ; 278 : 2563 - 2570
- 10 . van Dijk TH , Grefhorst A , Oosterveer MH . An increased flux through the glucose 6-phosphate pool in enterocytes delays glucose absorption in Fxr−/− mice . J Biol Chem . 2009 ; 284 : 10315 - 10323

- 11 . Duran-Sandoval D , Cariou B , Percevault F . The farnesoid X receptor modulates hepatic carbohydrate metabolism during the fasting-refeeding transition . J Biol Chem . 2005 ; 280 : 29971 - 29979
- 12 . Cariou B , van Harmelen K , Duran-Sandoval D . Transient impairment of the adaptive response to fasting in FXR-deficient mice . FEBS Lett . 2005 ; 579 : 4076 - 4080
- 13 . Ma K , Saha PK , Chan L . Farnesoid X receptor is essential for normal glucose homeostasis . J Clin Invest . 2006 ; 116 : 1102 - 1109
- 14 . Stayrook KR , Bramlett KS , Savkur RS . Regulation of carbohydrate metabolism by the farnesoid X receptor . Endocrinology . 2005 ; 146 : 984 - 991
- 15 . Rizzo G , Disante M , Mencarelli A . The farnesoid X receptor promotes adipocyte differentiation and regulates adipose cell function in vivo . Mol Pharmacol . 2006 ; 70 : 1164 - 1173
- 16 . Abdelkarim M , Caron S , Duhem C . The Farnesoid X Receptor Regulates Adipocyte Differentiation and Function by Promoting Peroxisome Proliferator-activated Receptor-{gamma} and Interfering with the Wnt/{beta}-Catenin Pathways . J Biol Chem . 2010 ; 285 : 36759 - 36767
- 17 . Thomas C , Pellicciari R , Pruzanski M . Targeting bile-acid signalling for metabolic diseases . Nat Rev Drug Discov . 2008 ; 7 : 678 - 693
- 18 . Watanabe M , Houten SM , Mataki C . Bile acids induce energy expenditure by promoting intracellular thyroid hormone activation . Nature . 2006 ; 439 : 484 - 489
- 19 . Katsuma SEA . Bile acids promote glucagon-like peptide-1 secretion through tgr5 in a murine enteroendocrine cell line stc-1 . Biochem Biophys Res Commun . 2005 ; 329 : 386 - 390
- 20 . Thomas C , Gioiello A , Noriega L . TGR5-mediated bile acid sensing controls glucose homeostasis . Cell Metab . 2009 ; 10 : 167 - 177
- 21 . Staels B , Handelsman Y , Fonseca V . Bile acid sequestrants for lipid and glucose control . Curr Diab Rep . 2010 ; 10 : 70 - 77
- 22 . Chen L , McNulty J , Anderson D . Cholestyramine reverses hyperglycemia and enhances GLP-1 release in Zucker Diabetic Fatty rats . J Pharmacol Exp Ther . 2010 ; 334 : 164 - 170
- 23 . Shang Q , Saumoy M , Holst JJ . Colesevelam improves insulin resistance in a diet-induced obesity (F-DIO) rat model by increasing the release of GLP-1 . Am J Physiol Gastrointest Liver Physiol . 2010 ; 298 : G419 - 24
- 24 . Murphy GM , Billing BH , Baron DN . A fluorimetric and enzymatic method for the estimation of serum total bile acids . J Clin Pathol . 1970 ; 23 : 594 - 598
- 25 . Elia M , Livesey G . Energy expenditure and fuel selection in biological systems: the theory and practice of calculations based on indirect calorimetry and tracer methods . World Rev Nutr Diet . 1992 ; 70 : 68 - 131
- 26 . Laskewitz AJ , van Dijk TH , Bloks VW . Chronic prednisolone treatment reduces hepatic insulin sensitivity while perturbing the fed-to-fasting transition in mice . Endocrinology . 2010 ; 151 : 2171 - 2178
- 27 . Popescu IR , Helleboid-Chapman A , Lucas A . The nuclear receptor FXR is expressed in pancreatic beta-cells and protects human islets from lipotoxicity . FEBS Lett . 2010 ; 584 : 2845 - 2851
- 28 . Chomczynski P , Sacchi N . Single-step method of RNA isolation by acid guanidinium thiocyanate-phenol-chloroform extraction . Anal Biochem . 1987 ; 162 : 156 - 159
- 29 . Laaksonen R , Katajamaa M , Päivä H . A systems biology strategy reveals biological pathways and plasma biomarker candidates for potentially toxic statin-induced changes in muscle . PLoS One . 2006 ; 1 : e97 -
- 30 . Kotronen A , Yki-Järvinen H . Fatty liver: a novel component of the metabolic syndrome . Arterioscler Thromb Vasc Biol . 2008 ; 28 : 27 - 38
- 31 . Zhang Y , Lee FY , Barrera G . Activation of the nuclear receptor FXR improves hyperglycemia and hyperlipidemia in diabetic mice . Proc Natl Acad Sci U S A . 2006 ; 103 : 1006 - 1011
- 32 . Biddinger SB , Kahn CR . From mice to men: insights into the insulin resistance syndromes . Annu Rev Physiol . 2006 ; 68 : 123 - 158
- 33 . Cipriani S , Mencarelli A , Palladino G . FXR activation reverses insulin resistance and lipid abnormalities and protects against liver steatosis in Zucker (fa/fa) obese rats . J Lipid Res . 2010 ; 51 : 771 - 784
- 34 . Gofflot F , Chartoire N , Vasseur L . Systematic gene expression mapping clusters nuclear receptors according to their function in the brain . Cell . 2007 ; 131 : 405 - 418

Figure 1

FXR-deficiency attenuates weight gain in ob/ob mice

A. $FXR^{+/+}$ ob/ob (white bars or diamonds) and $FXR^{-/-}$ ob/ob mice (black bars or triangles) (n=9–10/group) were monitored weekly for body weight. Significance of the overall effect of genotype ($p<0.0001$) and age ($p<0.0001$) as well as their interaction ($p<0.0001$) was calculated by 2way-ANOVA. **B.** Body composition was assessed by dual x-ray absorptiometry in twenty week old mice (n=9–10/group). **C.** O_2 -consumption (V_{O2}) and **D.** CO_2 -production (V_{CO2}) were determined in twenty week old mice (n=5/group) individually housed in metabolic cages. Values are means±SEM. Differences between genotypes over time were analyzed by 2way-ANOVA and Bonferroni post-hoc test, differences between genotypes were calculated by Mann-Whitney test (*0.05, **<0.01, ***<0.001).

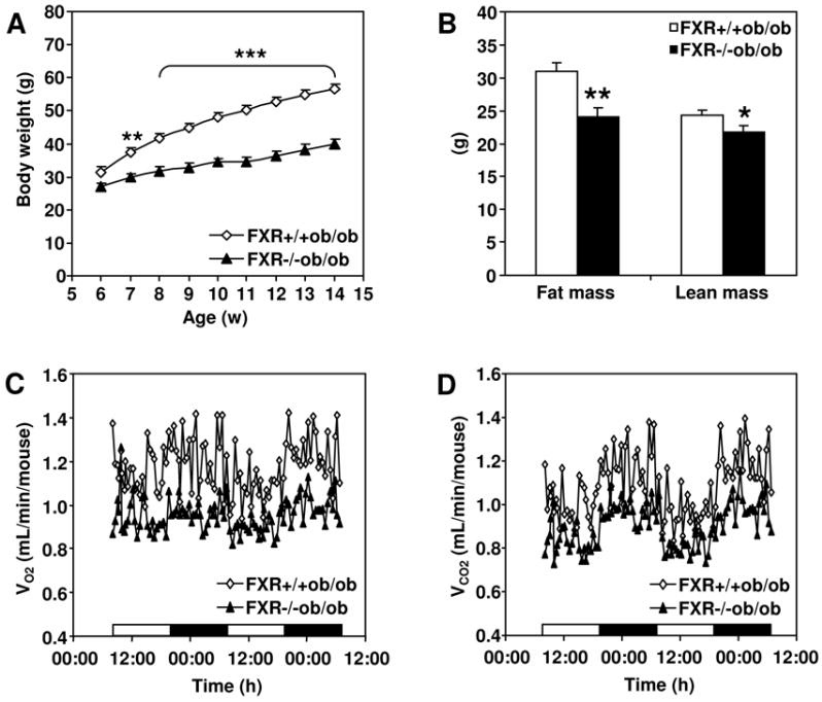

Figure 2

FXR-deficiency improves glucose homeostasis in ob/ob mice

A. Fasting blood glucose was measured weekly in $FXR^{+/+}$ ob/ob (white bars or diamonds) and $FXR^{-/-}$ ob/ob mice (black bars or triangles) (n =9–10/group). Significance of the overall effect of the genotype ($p<0.0001$) was calculated by 2way-ANOVA. **B.** Plasma insulin was determined in twelve week old mice (n=9–10/group). **C.** Blood glucose excursion and **D.** integrated AUC after administration of an i.p. glucose bolus (1g/kg glucose) were measured in twelve week old mice (n=9–10/group). Significance of the overall effect of genotype ($p<0.0001$) and time ($p<0.0001$) was calculated by 2way-ANOVA. **E.** Metabolic clearance rate (MCR) was determined by stable isotope dilution in fourteen week old mice (n=5–6/group). **F.** Blood glucose excursion and **G.** iAUC after administration of an i.p. insulin bolus (2IU insulin/kg) were measured in thirteen week old mice (n=9–10/group). Significance of the overall effect of genotype ($p<0.0001$) and time ($p<0.0001$) was calculated by 2way-ANOVA. **H.** Pancreases of twenty week old mice (n=9–10/group) were sectioned, submitted to Papanicolaou staining and **I.** the mean surface of the islets of Langerhans was quantified. Arrows indicate islets of Langerhans (scale bar = 1mm). Values are means±SEM. Differences between genotypes over time were analyzed by 2way-ANOVA and Bonferroni post-hoc test, differences between genotypes were calculated by Mann-Whitney test (*0.05, **<0.01, ***<0.001).

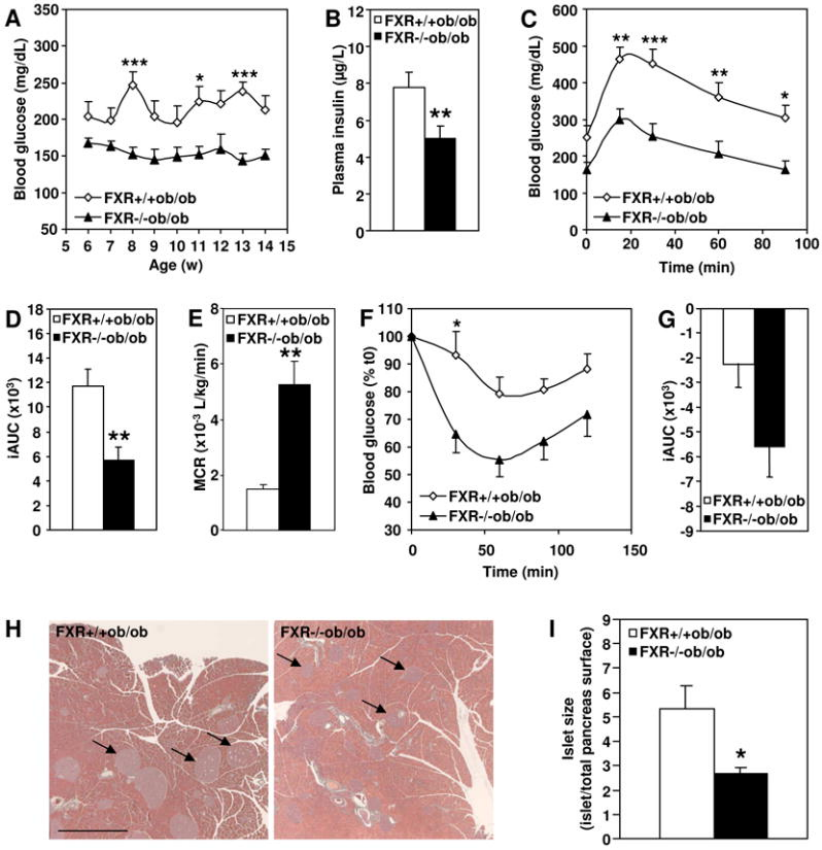

Figure 3

FXR-deficiency improves adipose tissue, but not hepatic insulin sensitivity in ob/ob mice

A. Thirteen week old female $FXR^{+/+}$ ob/ob (white bars) and $FXR^{-/-}$ ob/ob mice (black bars) (n=4/group) were injected with either saline or insulin. Phosphorylation of Akt at Serine473 and total Akt protein expression was determined by Western Blot and the signal quantified. **B.** Gene expression was measured by qPCR and **C.** triglyceride content was determined enzymatically in livers of twenty week old mice (n=9–10/group). Values are means±SEM. Differences between genotypes were calculated by Mann-Whitney test (*<0.05, **<0.01, ***<0.001). WAT, white adipose tissue; pAkt, Serine473-phosphorylated Akt; TG, triglyceride.

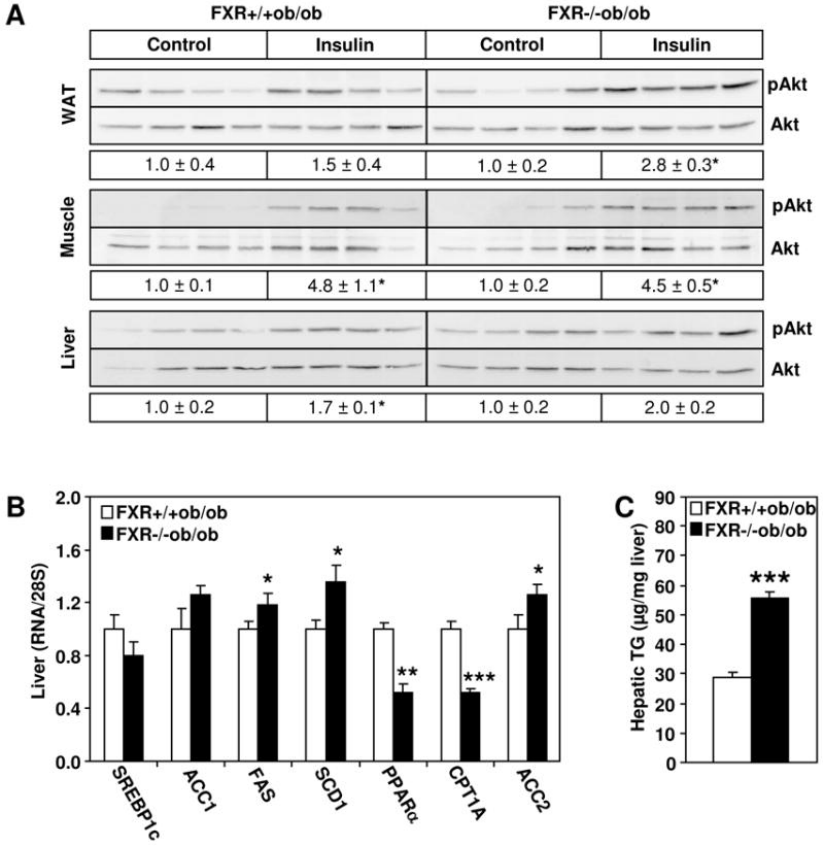

Figure 4

FXR-deficiency in ob/ob mice results in the accumulation of plasma triglycerides

A. and **B.** Lipid parameters were measured in plasma of twelve week old $FXR^{+/+}$ ob/ob (white bars or diamonds) and $FXR^{-/-}$ ob/ob mice (black bars or triangles) (n=9–10/group). **C.** Lipoprotein profiles were determined in plasma pools of thirteen week old mice. **D.** VLDL production was assessed in thirteen week old female mice (n=8–10/group) by measuring plasma triglyceride concentrations subsequent to Tyloxapol injection. **E.** Gene expression was measured by qPCR in livers of twenty week old mice (n=9–10/group). Values are means±SEM. Differences between genotypes were calculated by Mann-Whitney test (***<0.001). FFA, free fatty acid; TG, triglyceride; IDL, intermediary density lipoprotein.

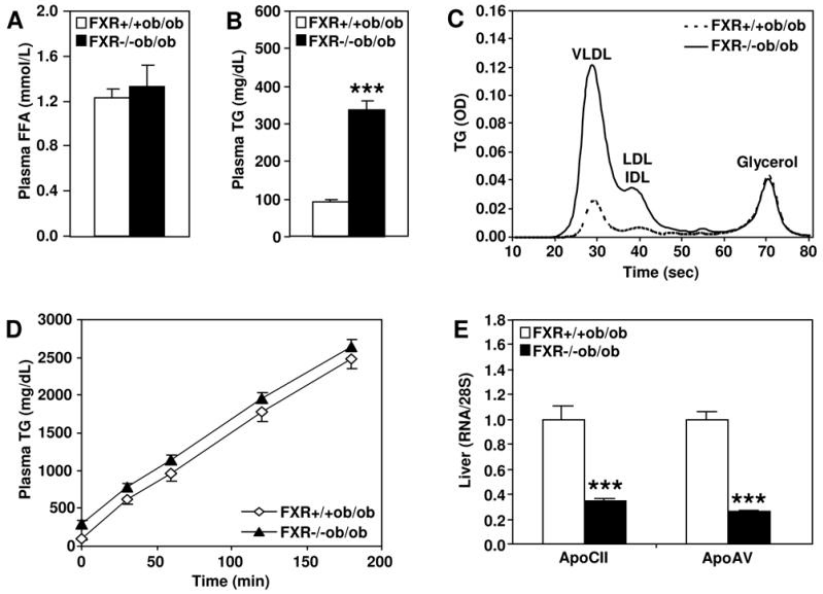

Figure 5

FXR-deficiency protects from diet-induced obesity and insulin resistance

$FXR^{+/+}$ (white bars or diamonds) and $FXR^{-/-}$ mice (black bars or triangles) (n=7–11/group) were fed a high-fat diet (HFD) for twenty weeks. **A.** Body weight was monitored weekly (n=7–11/group). Significance of the overall effect of genotype ($p<0.0001$) and age ($p<0.0001$) as well as their interaction ($p<0.0001$) was calculated by 2way-ANOVA. **B.** Plasma leptin, **C.** plasma TG, **D.** blood glucose and **E.** plasma insulin were determined at the end of the feeding period (n=4–9/group). **F.** Blood glucose excursion and **G.** integrated AUC after administration of an i.p. glucose bolus (1g/kg glucose) were measured at the end of the feeding period (n=6–9/group). Significance of the overall effect of genotype ($p<0.0001$) and time ($p<0.0001$) was calculated by 2way-ANOVA. Values are means±SEM. Differences between genotypes over time were analyzed by 2way-ANOVA and Bonferroni post-hoc test, differences between genotypes were calculated by Mann-Whitney test (* <0.05, **<0.01, ***<0.001). TG, triglyceride.

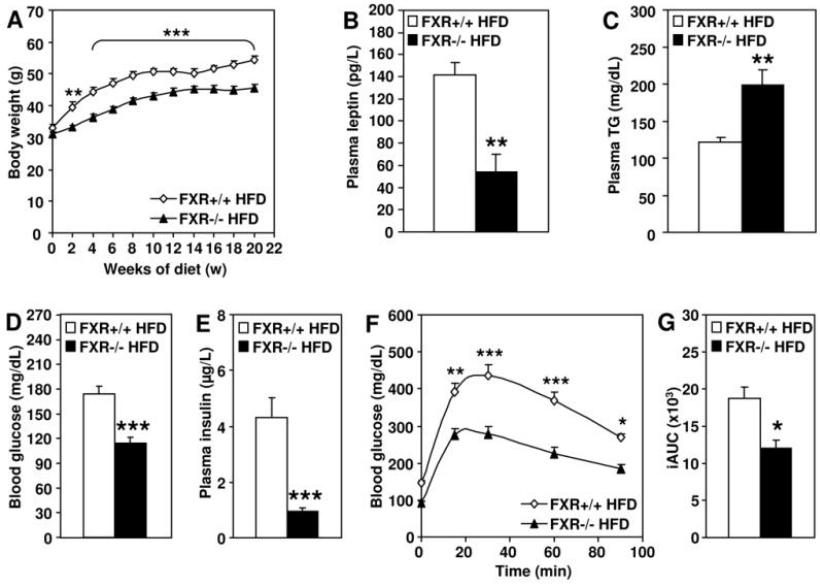

Figure 6

Liver-specific FXR-deficiency does not protect from diet-induced obesity and insulin resistance

LFXR$^{-/-}$ mice and LFXR$^{+/+}$ littermates (n=7–12/group) were fed a high-fat diet (HFD) or a control diet (CD) for ten weeks (LFXR$^{+/+}$ CD = vertically-hatched bars or circles; LFXR$^{-/-}$ CD = diagonally-hatched bars or squares; LFXR$^{+/+}$ HFD = white bars or diamonds; LFXR$^{-/-}$ HFD = black bars or triangles). **A.** Body weight was monitored weekly. Significance of the effect of diet ($p<0.0001$) and age ($p<0.0001$) as well as their interaction ($p<0.0001$) was calculated by 2way-ANOVA. **B.** Plasma leptin and **C.** plasma TG were determined at the end of the feeding period. **D.** Fasting blood glucose was measured weekly. Significance of the overall effect of diet ($p<0.0001$) and age ($p<0.0001$) as well as their interaction ($p=0.0217$) was calculated by 2way-ANOVA. **E.** Plasma insulin was measured after six weeks of feeding. **F.** Blood glucose excursion and **G.** integrated AUC after administration of an i.p. glucose bolus (1g/kg glucose) were measured after five weeks of feeding (n=6/group). Values are means±SEM. Differences between diet groups over time were analyzed by 2way-ANOVA and Bonferroni post-hoc test, differences between genotypes or diet groups were calculated by Mann-Whitney test (*compares genotypes of the same diet group; $ compares diet groups for LFXR$^{+/+}$; § compares diet groups for LFXR$^{-/-}$; $ or §<0.05, ** or $$ or §§ <0.01, $$$ or §§§<0.001). TG, triglyceride.

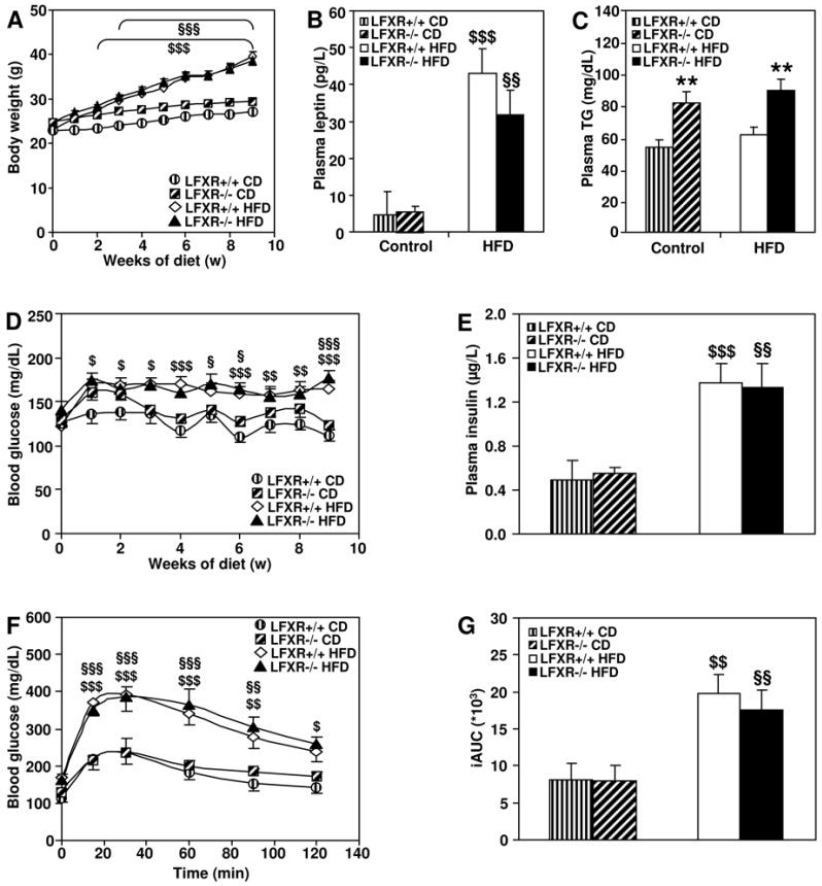

Figure 7

Modulation of bile acid metabolism does not affect glucose homeostasis in $FXR^{-/-}$ ob/ob mice

Ten week old $FXR^{+/+}$ ob/ob and $FXR^{-/-}$ ob/ob mice were administered 2% colesevelam mixed in the diet or plain diet for three weeks (n= 13/group) ($FXR^{+/+}$ ob/ob control = white bars or diamonds; $FXR^{+/+}$ ob/ob treated = vertically-hatched bars or circles; $FXR^{-/-}$ ob/ob control = black bars or triangles; $FXR^{-/-}$ ob/ob treated = diagonally-hatched bars or squares). **A.** TGR5 target gene expression was measured by qPCR in BAT of twenty week old mice (n=9–10/group). **B.** Plasma bile acids were measured after nine days of treatment. **C.** Body weight was monitored weekly during the treatment period. Significance of the overall effect of treatment ($p<0.0001$) and age ($p=0.0002$) was calculated by 2way-ANOVA. **D.** Fasting blood glucose was determined weekly during the treatment period. **E.** Blood glucose excursion and **F.** integrated AUC after administration of an i.p. glucose bolus (1g/kg glucose) were measured at the end of the treatment period. **G.** Plasma insulin was measured at the end of the treatment period. Values are means±SEM. Differences between treatment groups over time were analyzed by 2way-ANOVA and Bonferroni post-hoc test, differences between genotypes or treatment groups were calculated by Mann-Whitney test (*compares genotypes of the same treatment group; $ compares treatment groups of the same genotype; *or $<0.05, **or $$<0.01, ***or $$$≪0.001). BAT, brown adipose tissue; BA, bile acids.

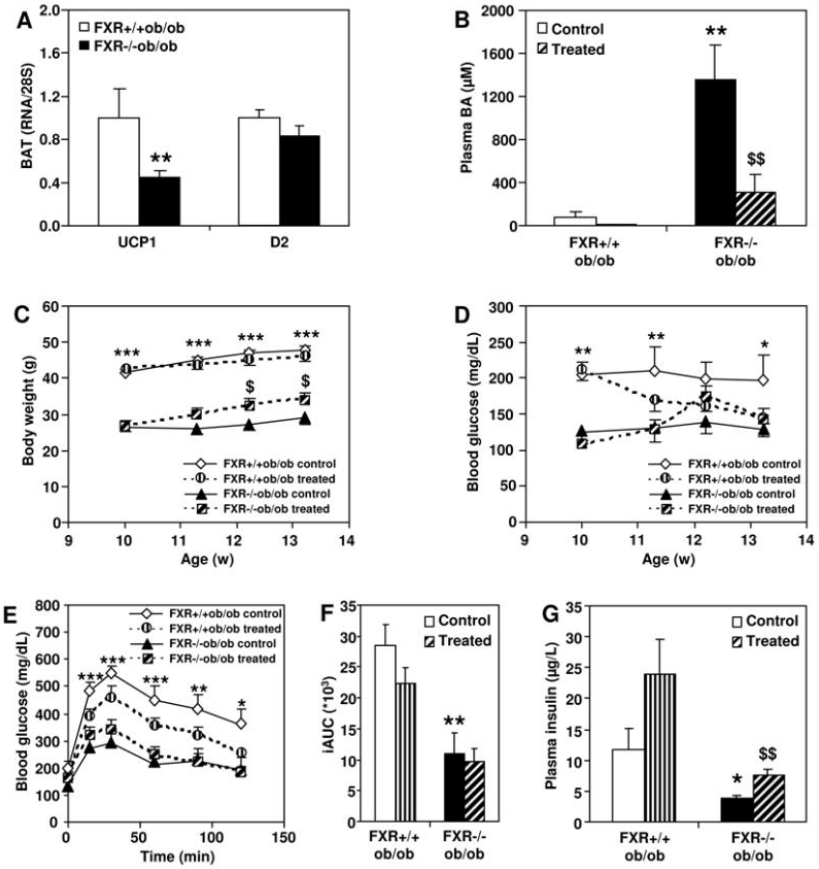

Figure 8

FXR-deficiency differentially affects the abundance of long-chain, unsaturated triglyceride species in adipose tissue of lean and obese mice

Lipidomics analysis was performed in white adipose tissue of six week old $FXR^{+/+}$ ob/ob, $FXR^{-/-}$ ob/ob mice as well as lean $FXR^{+/+}$ and $FXR^{-/-}$ littermates (Lean $FXR^{+/+}$ = white bars or vertically-hatched circles; Lean $FXR^{-/-}$ = black bars or diagonally-hatched squares; Obese $FXR^{+/+}$ = white bars or diamonds; Obese $FXR^{-/-}$ = black bars or triangles). Representative data for **A.–C.** medium-chain triglycerides with a high saturation level, **D.–F.** long-chain, highly unsaturated triglycerides and **G.–I.** long-chain triglycerides containing few double-bounds. **J.** PLS/DA of all measured lipid species. Values are means±SEM. Differences between genotypes were calculated by 1way-ANOVA and Student's t-test (*compares the effect of leptin-deficiency; $ compares the effect of FXR-deficiency; *or $<0.05, **or $$<0.01, ***or $$$ <0.001). TG, triglyceride; LV, latent variable.